many different initial pressures of $H_2(g)$ and $C_2H_4(g)$. In the particular experiment shown, $P^{\circ}_{C_2H_4}$ was held constant while $P^{\circ}_{H_2}$ was varied in each experiment to determine the kinetic order with respect to H_2. The initial pressure decrease with time, $[\Delta P(t)]$, is usually linear, or very nearly so, in the first 3 to 4 s and is used as a measure of the initial rate of the hydrogenation reaction. Departures from linearity after ~5 s are due mainly to the consumption of reactants. We are confident that in the first few seconds of the reaction, diffusion of reactants through the gas phase to the catalyst surface is not a significant rate-controlling factor, based on control experiments which will be discussed shortly.

Data such as that in the bottom panel of Figure 10 can be treated by the following analysis of the linear least-squares derived initial slope. The stoichiometry of the reaction, 2 mol → 1 mol, makes the pressure a convenient method of monitoring the rate. The initial rate is given by eq 6, where $dN_{C_2H_6}/dt$ = molecules·s^{-1},

$$\text{rate}_i = R_i = \left(\frac{dN_{C_2H_6}}{dt}\right)_i = -\frac{V_{Tot}\cdot N_A}{RT}\frac{dP_i}{dt} \qquad (6)$$

and dP_i/dt = initial slope. The initial slope has units torr·s^{-1}; V_{tot} = 299.2 cm^3; N_A is Avogadro's number; R = 6.236 × 10^4 cm^3·torr·mol^{-1}·K^{-1}; and T is the temperature in Kelvin. The initial rate is then given in molecules·s^{-1}, with typical values in the 10^{16} to 10^{17} molecule·s^{-1} range (~3.1 × 10^{13} molecule·cm^{-2}·s^{-1}). Our conservative estimate of the precision by this technique is ±6%, with the largest contribution being due to our inability to precisely determine $\Delta P(t)$ in the region of steepest slope (see Figure 10).

We have conducted experiments to determine if our measured rates are being limited by the diffusion of reactants to the surface. By keeping the initial pressures of $H_2(g)$ and $C_2H_4(g)$ equal and constant at 0.0500 torr and increasing the initial pressure of N_2 which is added along with the $C_2H_4(g)$ + $H_2(g)$, the effect on the kinetics from diffusion of reactants through background $N_2(g)$ was checked. These data are shown in Figure 11. There is clearly no strong functional dependence of the measured initial rate on the total pressure at these pressures. Even for experiment 6, where 60% of the initial gas phase is composed of N_2, there is no apparent effect of diffusion through the $N_2(g)$ on the measured rate. This result, in conjunction with the fact that all rate measurements were made at H_2 + C_2H_4 total gas pressures ≤0.250 torr, is strong evidence that our measured rates are not being limited by diffusion of reactants through the gas phase to the catalyst surface.

IR Transition Moment Directions in Matrix-Isolated Dimethylsilylene and 1-Methylsilene

Gerhard Raabe,[1a,b] H. Vančik,[1a] Robert West,[1c] and Josef Michl*[1a]

Contribution from the Departments of Chemistry, University of Utah, Salt Lake City, Utah 84112, and University of Wisconsin—Madison, Madison, Wisconsin 53706. *Received July 23, 1985*

Abstract: Irradiation of matrix-isolated dimethyldiazidosilane yields dimethylsilylene (**1**) as the major product. Photoselection on the 450-nm absorption band of **1** with polarized 488-nm light, which converts **1** into 1-methylsilene (**2**), permitted the assignment of six IR transitions of **1** and twelve IR transitions of **2** as in-plane or out-of-plane polarized. Photoselection on the 260-nm absorption band of **2** with polarized 248-nm light, which converts **2** back into **1**, allowed a determination of the absolute values of polarization angles of seven in-plane polarized IR transitions of **2** relative to the $\pi\pi^*$ transition moment. The resulting map of the IR transition moment directions in the molecule of **1** provides strong support for the detailed assignment of the nature of the vibrational motions involved. Along with other data, the results leave very little doubt as to the correctness of the structural and vibrational assignments in **1** and **2**.

Although Turner and collaborators[2] have demonstrated the power of the combined use of UV-visible photoselection and IR linear dichroism on molecules isolated in rare-gas matrices, the procedure has seen only limited further development. We now wish to report (i) its qualitative use to extend the symmetry assignments of the vibrations of dimethylsilylene (**1**) from two[3] to six fundamentals and (ii) its quantitative use to determine the polarization directions of twelve fundamental vibrations of 1-methylsilene (**2**), previously[3] only characterized as in-plane or out-of-plane polarized. To our knowledge, this is the first determination of IR polarization angles on a matrix-isolated molecule of low (C_s) symmetry.

The choice of **1** and **2** for targets of a detailed IR investigation was motivated in part by the still novel nature of the Si=C moiety, whose force field is of considerable interest.[3,4] In addition, it appears desirable to establish the identity and spectral properties of matrix-isolated **1** and **2** in an unassailable fashion in response to the recently raised doubts.[5,6] We have summarized the arguments in favor of the original assignments[3,7-9] elsewhere.[10] In our judgment, the evidence now is quite overwhelming.

The great improvement in the signal-to-noise ratio in the presently obtained dichroic spectra relative to prior work[3] was made possible by the use of dimethyldiazidosilane as a photochemical precursor[10] for **1**. The mechanism of the multistep

(1) (a) University of Utah. (b) Presented at the XIX Organosilicon Symposium, Louisiana State University, Baton Rouge, LA, April 26 and 27, 1985. (c) University of Wisconsin—Madison.

(2) E.g.: Burdett, J. K.; Grzybowski, J. M.; Perutz, R. N.; Poliakoff, M.; Turner, J. J.; Turner, R. F. *Inorg. Chem.* **1978**, *17*, 147. Church, S. P.; Poliakoff, M.; Timney, J. A.; Turner, J. J. *J. Am. Chem. Soc.* **1981**, *103*, 7515.

(3) Arrington, C. A.; Klingensmith, K. A.; West, R.; Michl, J. *J. Am. Chem. Soc.* **1984**, *106*, 525.

(4) Schlegel, H. B.; Wolfe, S.; Mislow, K. *J. Chem. Soc., Chem. Commun.* **1975**, 246. Baskir, E. G.; Maltsev, A. K.; Nefedov, O. M. *Izv. Akad. Nauk SSSR, Ser. Khim* **1983**, 1314. Maltsev, A. K.; Khabashesku, V. N.; Nefedov, O. M. *J. Organomet. Chem.* **1984**, *271*, 55.

(5) Hawari, J. A.; Griller, D. *Organometallics* **1984**, *3*, 1123.

(6) Nazran, A. S.; Hawari, J. A.; Griller, D.; Alnaimi, I. S.; Weber, W. P. *J. Am. Chem. Soc.* **1984**, *106*, 7267.

(7) Drahnak, T. J.; Michl, J.; West, R. *J. Am. Chem. Soc.* **1979**, *101*, 5427.

(8) Drahnak, T. J.; Michl, J.; West, R. *J. Am. Chem. Soc.* **1981**, *103*, 1845.

(9) Maier, G.; Mihm, G.; Reisenauer, H. P.; Littmann, D. *Chem. Ber.* **1984**, *117*, 2369.

(10) Vančik, H.; Raabe, G.; Michalczyk, M. J.; West, R.; Michl, J. *J. Am. Chem. Soc.* **1985**, *107*, 4097.

0002-7863/86/1508-0671$01.50/0

photochemical process in which **1** is produced and the generality of this approach to silylenes are presently under investigation.

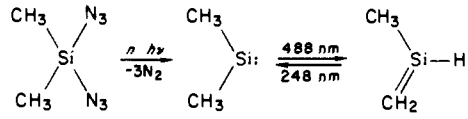

1 2

Experimental Section

Matrices were made by condensing argon containing ~0.3% dimethyldiazidosilane (Petrarch) on a CsI window cooled by an Air Products closed-cycle helium cryostat. During the deposition the temperature was held at 25 K. Deposition rates for the gas mixture were up to ~0.5 mmol/min. Lower deposition rates did not lead to matrices of higher optical quality. Irradiation and spectral measurements were done at 10–14 K. Complete destruction of the dimethyldiazidosilane and production of dimethylsilylene took 12–24 h of irradiation with unfiltered light of a low-pressure mercury lamp (Ultraviolet Products, Inc.) through a quartz window, depending on the thickness of the matrix. In some experiments, nitrogen, krypton, or xenon matrices were used as well. Deposition conditions were optimized for each gas separately in order to obtain clear matices (~50 K window temperature for xenon). For irradiation and measurement, the matrices were always cooled to 10–14 K. In most cases this caused cracking, but the resulting increase in light scattering was tolerable.

Randomly oriented 1-methylsilene samples were produced by bleaching the dimethylsilylene with the visible emission of a high-pressure Xe lamp, obtained with use of a UV cutoff filter. Partially oriented samples of 1-methylsilene and dimethylsilylene were obtained (i) from randomly oriented matrix-isolated dimethylsilylene by irradiation with the highly polarized 488-nm line (200 mW) of an SP-165-6 Spectra Physics Ar^+ laser (photoselection on the visible band of **1**) and (ii) from randomly oriented 1-methylsilene by irradiation with the 248-nm light of a KrF excimer laser (Lambda Physik, average power 300 mW), polarized by a Glan-Thompson polarizer (photoselection on the UV band of **2**).

IR spectra were recorded on a Nicolet 6000 series FT IR spectrometer with 1-cm^{-1} resolution (300 scans). Polarized infrared spectra (at least 1000 scans) were recorded using an IPG-225 aluminum grid polarizer (Cambridge Physical Sciences, Ltd.).

UV–visible spectra were taken on a Cary-17D UV–visible spectrometer equipped with Glan-Thompson polarizers.

Results and Discussion

Ordinary Spectra. Irradiation of matrix-isolated dimethyldiazidosilane with 254-nm light causes a rapid disappearance of its characteristic bands in the IR spectrum (Figure 1). The intense antisymmetric N_3 stretching band pair near 2150 cm^{-1} is first replaced by a single new band, presumably due to a product with only one azido group, which then diminishes in its turn until essentially all absorption in this characteristic region disappears. There are indications in the spectra that additional intermediates may be formed and destroyed before the essentially azide-free IR spectrum shown in the center part of Figure 1 is obtained. The absorption intensity in this spectrum is far weaker than that in the starting one (note the difference in scales). The spectrum contains all the IR peaks previously assigned[3,7-9] to dimethylsilylene (**1**). Additional peaks, absent in the spectra of **1** obtained from other precursors,[3,7-9] are also present and are particularly noticeable in the saturated Si—H and CH_2=N stretching regions. These are presumably due to side products and possibly also to incompletely photolyzed intermediates. At least some of the side products are apparently related in structure to the product obtained by the irradiation of matrix-isolated trimethylsilylazide,[11] Me_2HSi—N=CH_2. They are of limited interest in the present context.

At this point, the originally colorless matrix is deep yellow and its UV–visible spectrum shows the characteristic broad absorption band at 450 nm previously assigned[3,7-9] to **1**. Next, one can take advantage of the known[3,8,9] sensitivity of **1** to visible light in order to separate its IR spectrum from those of the other materials present. Irradiation of the matrix with visible light causes a concurrent decrease of all the IR bands and of the visible band

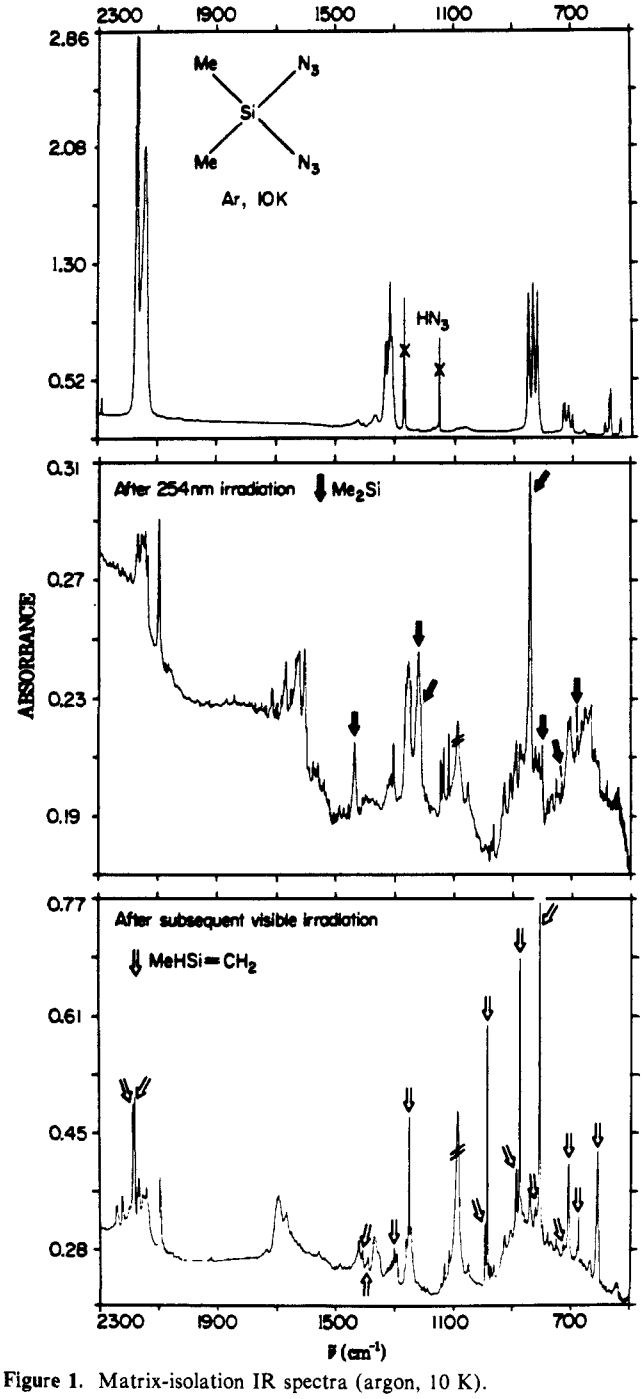

Figure 1. Matrix-isolation IR spectra (argon, 10 K).

assigned to **1** and of a few of those attributed to the side products. Simultaneously, it leads to the growth of a new set of IR bands which have been previously attributed[3,8,9] to 1-methylsilene **2** and of a few others. Concurrently, a new UV band appears near 260 nm. This has also been previously assigned[3,8,9] to **2**. Finally, the matrix loses the yellow color and has the IR spectrum shown in the bottom part of Figure 1. Most of the IR peaks attributed to the side products are not affected by visible irradiation.

Subsequent irradiation of the colorless matrix with 248-nm light reverses the process: the IR peaks of **2** gradually disappear while the IR and visible bands of **1** grow in. The cycle has been repeated four times without obvious signs of fatigue on the part of the matrix. Within the inaccuracies dictated by base line uncertainties, the intensities of the IR bands of **1** remain proportional to that of its UV–visible band throughout. This appears to be true of **2** also, but the short wavelength of its UV band makes a quantitative assessment far more difficult.

Computer subtraction of the spectra of the matrix in its yellow and colorless forms causes a cancellation of all peaks which do

(11) Perutz, R. N. *J. Chem. Soc., Chem. Commun.* **1978**, 762.

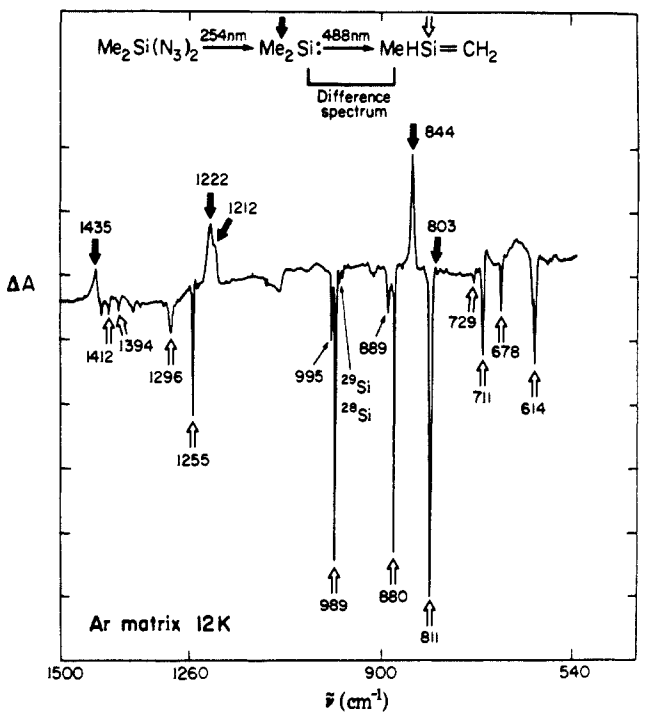

Figure 2. IR difference spectrum of an argon matrix containing **1** before (positive) and after (negative) bleaching with visible light (10 K).

not respond to visible nor UV irradiation. Repeated experiments of this kind permitted us to extract the best IR spectra of **1** and **2** that we have yet obtained from any precursor. The positions of peaks in both spectra agree very well with those reported previously with other precursors.[3,7-9] The relative intensities of a few peaks at **1** and **2** which were either too weak or too strongly overlapped to be seen previously[3,7-9] have now been observed to track faithfully those of all the other bands and can be added to the list; a few frequencies can be determined more accurately than before. The results are summarized in Table I (**1**) and II (**2**), comparable to Table I and II of ref 3, respectively. An example of a difference spectrum is shown in Figure 2.

Several of the strongest IR bands of **2** have satellites whose relative intensity is a function of the choice of the matrix material and of the details of the experimental procedure and which were not observed previously with other precursors. They are listed in parentheses in Table II. We believe that they are due to a site effect and are caused by molecules whose environment differs in some way, such as the number of neighboring nitrogen molecules.

In nitrogen, krypton, and xenon matrices the spectra of **1** and **2** are very similar to those observed in argon, including the weak IR satellites. The most noticeable difference is a shift of the visible band of **1** which appears at 430 nm in N_2, 450 nm in Ar, 455 nm in Kr, and 470 nm in Xe. The origin of these shifts is not clear. They are not in the order one would expect if electron donation into the vacant p orbital on silicon by the matrix atoms were the dominant factor. They may be due to small changes in the CSiC valence angle in **1** dictated by the packing forces, since one can expect the excitation energy to be a sensitive function of the degree of hybridization on silicon. We have tried to obtain evidence for this by investigating the relative intensities of the symmetric and antisymmetric combination of the Si–C stretches as a function of the matrix material, but this effort failed because of the weakness of these IR bands.

Photoselection[12,13] on the Visible Band of 1. In these experiments, **1** was partially bleached with linearly polarized visible light

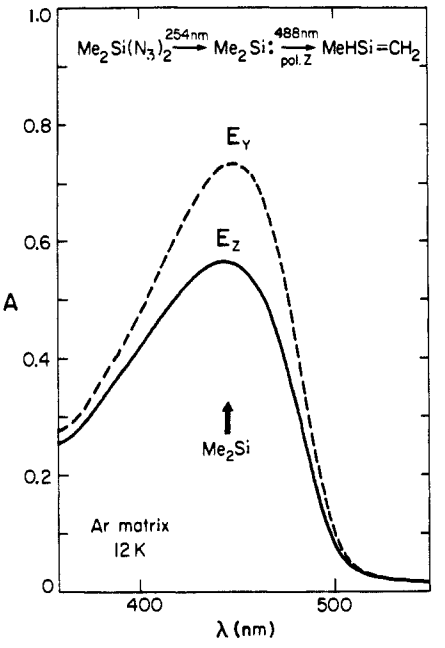

Figure 3. Polarized visible spectra of argon-matrix-isolated **1** partially converted to **2** with the *Z*-polarized 488-nm line of an Ar^+ laser (10 K). E_Z (E_Y): absorbance polarized along *Z* (*Y*).

whose electric vector was directed along the laboratory axis *Z*. The polarized IR and UV–visible spectra E_Z and E_Y were then taken with light polarized along *Z* and *Y*, respectively. The contributions due to species other than **1** and **2** were first removed by computer subtraction as described above. Then, the dichroic ratio $d_i = E_Z(i)/E_Y(i)$ was determined for each transition *i* and the difference spectra $E_Z - E_Y$ were plotted. Figure 3 shows the visible spectra E_Z and E_Y; Figure 4 shows an example of the difference IR spectra $E_Z - E_Y$ obtained at two different degrees of conversion. Since they are double difference spectra, they tend to be quite noisy. They were taken many times at various degrees of conversion and only the features which were reproducibly present are indicated by arrows in Figure 4. The orientation of **2** is highest at low degrees of conversion and that of **1** at high degrees of conversion, i.e., just when their respective concentrations are the smallest, so that a suitable compromise needs to be found for optimal results. For the weakest among the IR peaks of **1** and **2**, the dichroic ratio and in a few cases even the sign of the dichroism could not be determined reliably in spite of repeated efforts.

Assuming that the absorbing transition in **1** is of the n → p type as in SiH_2 itself,[14] and as suggested by our INDO/S calculations, its polarization is perpendicular to the CSiC plane. The symmetry axis in **1** is labeled *z*. The symmetry labels in Table I of ref 3 were based on *y* being perpendicular to the CSiC plane and *x* lying in this plane. This has now been changed to the currently more common usage, *y* in-plane and *x* out-of-plane (Table I). Therefore, the b_1 and b_2 labels are now interchanged relative to ref 3.

Photoselection on the *x*-polarized visible transition of **1** will leave behind an assembly partially oriented with *x* perpendicular to *Z* and the *y*,*z* (CSiC) plane aligned with *Z*. Transitions into states of b_1 symmetry (*x* polarized) will therefore exhibit negative dichroism ($E_Z < E_Y$) with a constant dichroic ratio $d_x < 1$. Transitions into states of either a_1 or b_2 symmetry (*z* and *y* polarized, respectively) will exhibit positive dichroism ($E_Z > E_Y$) with a constant dichroic ratio $d_y = d_z > 1$, related to d_x by $d_y = 2/(1 + d_x)$.

This relation between d_x, d_y, and d_z is perhaps most readily derived by using the "orientation factors" of the molecular axes K_u ($u = x, y, z$), familiar from from the analysis of linear dichroism

(12) Albrecht, A. C. *J. Mol. Spectrosc.* **1961**, *6*, 84. Dörr, F. In "Creation and Detection of the Excited State"; Lamola, A. A., Ed.; Marcel Dekker: New York, 1971; Vol. 1, Chapter 2.

(13) Michl, J.; Thulstrup, E. "Spectroscopy with Polarized Light. Solute Alignment by Photoselection, Liquid Crystals, Polymers, and Membranes"; VCH Publishers, Inc.: Deerfield Beach, FL, 1986.

(14) Dubois, I.; Herzberg, G.; Verma, R. D. *J. Chem. Phys.* **1967**, *47*, 4262. Bürger, H.; Eujen, R. *Top. Curr. Chem.* **1974**, *50*, 19.

Table I. Dimethylsilylene Vibrations

		calculated (MNDO)[3]				previous observation[3]			present observation		
		$\tilde{\nu}$ (cm^{-1})	int. (cm^2 mol^{-1})		assignment[a]	$\tilde{\nu}$ (cm^{-1})	int.[b]	polarization	$\tilde{\nu}$ (cm^{-1})	int.[b]	polarization
1	ν_1	3335	4	a_1	CH_3 stretch						
2	ν_{16}	3334	3	b_2	CH_3 stretch						
3	ν_2	3261	307	a_1	CH_3 stretch				2977	s	
4	ν_{17}	3260	330	b_2	CH_3 stretch				2942	m	
5	ν_{12}	3256	592	b_1	CH_3 stretch						
6	ν_8	3254	0	a_2	CH_3 stretch						
7	ν_{13}	1442	37	b_1	a CH_3 def	1435	m		1435	m	out-of-plane
8	ν_9	1439	0	a_2	a CH_3 def						
9	ν_3	1431	48	a_1	a CH_3 def						
10	ν_{18}	1429	23	b_2	a CH_3 def						
11	ν_4	1394	1300	a_1	s CH_3 def	1220	s	in-plane	1222	s	in-plane
12	ν_{19}	1389	1515	b_2	s CH_3 def	1210	m	in-plane	1212	s	in-plane
13	ν_5	841	5870	a_1	in-plane CH_3 rock	850	s		844	vs	in-plane
14	ν_{20}	831	8870	b_2	in-plane CH_3 rock	806	vs		803	w	in-plane
15	ν_6	754	566	a_1	Si–C stretch	690	m		690	w	in-plane
16	ν_{21}	699	424	b_2	a Si–C stretch	735	m		*c*		
17	ν_{10}	635	0	a_2	out-of-plane CH_3 rock						
18	ν_{14}	608	21	b_1	out-of-plane CH_3 rock						
19	ν_7	293	1635	a_1	C–Si–C bend						
20	ν_{15}	0.1	14	b_1	torsion						
21	ν_{11}	0.03	0	a_2	torsion						

[a] See ref 3 for a discussion of the assignments (there, b_1 and b_2 labels are interchanged relative to the present convention). [b] The classification of relative peak intensities as strong (s), medium (m), and weak (w) is somewhat subjective and the labels are affected by the bandwidth which may vary depending on the precursor used. In a sense, all of the eight observed peaks should be listed as strong. [c] The 735-cm^{-1} band has not been observed with the $Me_2Si(N_3)_2$ precursor, either because it is broader or because it does not belong to Me_2Si.

Table II. 1-Methylsilene Vibrations

		calculated (MNDO)[3]			calculated (MNDO, planarity enforced[18])			previous observation[3]			present observation					
		$\tilde{\nu}$ (cm^{-1})		asignment[a]	$\tilde{\nu}$ (cm^{-1})	int. (km mol^{-1})	polarization	$\tilde{\nu}$ (cm^{-1})	int.[b]	polarization	$\tilde{\nu}$ (cm^{-1})	int.[b]	polarization	K,[c]	α_z(i)[d]	α_z(ii)[d]
1	ν_1	3413	a′	s CH_2 stretch	3427	13.7	+1°				3018	w	*f*			
2	ν_2	3383	a′	a CH_2 stretch	3396	11.8	−89°									
3	ν_3	3351	a′	s CH_3 stretch	3354	6.5	+59°				2976	w	*f*			
4	ν_4	3287	a′	a CH_3 stretch	3289	13.4	+34°									
5	ν_{15}	3277	a″	a CH_3 stretch	3283	11.0	a″									
6	ν_5	2280	a′	Si–H stretch	2294	47.3	−62°	2188	s	in-plane	2182, 2187	s	in-plane	0.38	90°	90°
7	ν_{16}	1433	a″	a CH_3 def	1430	10.0	a″	1412	m		1412	w	out-of-plane			
8	ν_6	1429	a′	a CH_3 def	1427	12.3	+89°	1397	m		1394	w	in-plane			
9	ν_7	1425	a′	CH_2 scissor	1422	44.6	+7°	1300	m		1296	w	in-plane	0.26	(−)22°	0°
10	ν_8	1384	a′	CH_3 def	1383	60.0	+50°	1254	s	in-plane	1255	s	in-plane	0.36	(+)68°	(+)72°
11	ν_9	1049	a′	Si=C stretch	1078	17.9	+6°	988	s	in-plane	(996),[e] 989	s	in-plane	0.28	(−)32°	(−)25°
12	ν_{17}	992	a″	CH_2 out-of-plane wag	994	0.7	a″	830	s		831	w	out-of-plane			
13	ν_{10}	863	a′	CH_2 + SiH in-plane bend	882	20.8	+3°	880	s	in-plane	(889)[e],880	s	in-plane	0.30	(+)41°	(+)37°
14	ν_{11}	831	a′	in-plane CH_3 rock	833	17.9	−56°	812	vs	in-plane	(801)[e],811	s	in-plane	0.39	90°	90°
15	ν_{18}	769	a″	out-of-plane CH_3 rock	772	5.0	a″	714	m	out-of-plane	711	m	out-of-plane			
16	ν_{12}	747	a′	Si–C stretch	754	22.1	−62°	732	m	in-plane	729	w	*f*			
17	ν_{13}	681	a′	SiH + CH_2 in-plane bend	689	15.4	+26°	688	w	in-plane	678	m	in-plane	0.29	(+)37°	(+)31°
18	ν_{19}	599	a″	CH_2 twist + SiH out-of-plane bend	609	15.5	a″	615	m	out-of-plane	614	m	out-of-plane	0.38	90°	90°
19	ν_{20}	329	a″	SiH out-of-plane bend + CH_2 twist	(241i)											
20	ν_{14}	224	a′	C–Si–C bend	253	9.2	+66°									
21	ν_{21}	46	a″	CH_3 torsion	25	3.6	a″									

[a] See ref 3 for a discussion of the assignments. [b] See footnote *b* in Table I. [c] The orientation factor K was obtained from the observed dichroic ratio $d = E_Z/E_Y$ using $K = d/(d + 2)$. [d] The angle between the IR transition and the $\pi\pi^*$ transition moment direction, measured counterclockwise in Figure 6. The signs in parentheses are not experimental but are chosen to agree with theory. The two choices of K values are labeled (i) and (ii), see text. [e] Weak satellites (see text). [f] This transition was too weak to obtain reliable dichroic data.

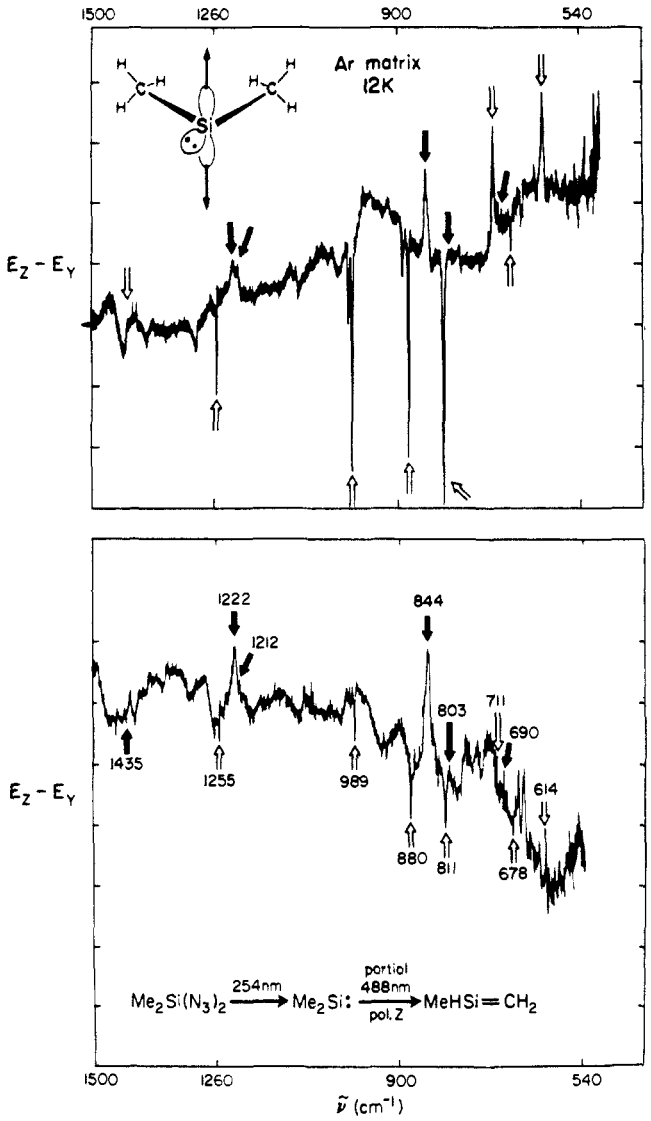

Figure 4. Polarized IR difference spectrum of argon-matrix-isolated **1** (dark arrows) partially converted to **2** (light arrows) with the *Z*-polarized 488-nm line of an Ar^+ laser (10 K). Top, small degree of conversion; bottom, larger degree of conversion.

of samples embedded in stretched polymers.[13,15] These are defined as $K_u = \langle \cos^2 u \rangle$, where u is the angle between *Z* and the molecular axis *u* and the brackets indicate averaging. In uniaxial samples, they are related to the observed dichroic ratios d_u by $d_u = 2K_u/(1 - K_u)$. From the properties of direction cosines, $K_x + K_y + K_z = 1$; since $K_y = K_z$ in the present case, the above relation between d_x and d_y follows.

Experimentally, we observed the expected negative dichroism for the visible band of **1** (Figure 3). In the IR, only the 1435-cm^{-1} peak showed negative dichroism, confirming its assignment[3] to an out-of-plane polarized vibration (b_1 antisymmetric methyl deformation). The peaks at 690, 803, 844, 1212, and 1222 cm^{-1} showed positive dichroism, confirming their assignment to in-plane polarized a_1 or b_2 vibrations (Table I). The degree of alignment increased with the advancing degree of photoconversion, as it should. Within the relatively low experimental accuracy (Figure 4), the values of the dichroic ratios behaved according to expectations.

The photoselective transformation of **1** into **2** also has the potential of producing a partially aligned assembly of product molecules **2**. Whether this will be realized depends on the behavior

(15) Thulstrup, E. W.; Michl, J. *J. Phys. Chem.* **1980**, *84*, 82. Thulstrup, E. W.; Michl, J. *J. Am. Chem. Soc.* **1982**, *104*, 5594. Radziszewski, J. G.; Michl, J. *J. Am. Chem. Soc.*, in press.

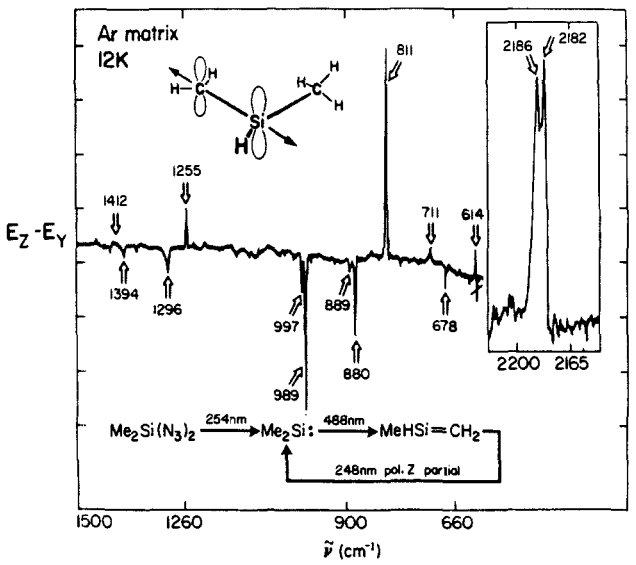

Figure 5. Polarized IR difference spectrum of argon-matrix-isolated **2** (light arrows) partially converted to **1** with the *Z*-polarized 248-nm line of a KrF excimer laser (10 K).

of the product molecules after they are formed. If they have sufficient excess vibrational and rotational energy they may undergo more or less indiscriminate rotations out of their initial orientation and lose most or all memory of their initial spatial relation to *Z*. In an extreme case, an unoriented sample of **2** will result. On the contrary, if they possess no excess energy that would allow them to soften the environment and move relative to it, a partially oriented sample of **2** will be obtained. In this limit, transitions into *x*-polarized states (polarized perpendicular to the CSiC plane) will then exhibit positive dichroism, $d_x > 1$. Transitions polarized along any direction perpendicular to *x*, i.e., in the CSiC plane, will all exhibit the same negative dichroism, with $d = 2/(1 + d_x)$. Intermediate cases may be encountered, and in particular, if the rotational relaxation is incomplete but anisotropic, transitions polarized along different directions perpendicular to *x* need not all have the same dichroic ratio *d*.

Experimentally, we observed a behavior corresonding to the second limit: the product **2** was partially oriented (Figure 4) and its peaks showed one of two dichroic ratios, related as expected.

The peaks at 614, 711, 1412, and, less distinctly, 831 cm^{-1} showed positive dichroism as expected from their assignment[3] to a″ vibrations; eight others showed negative dichroism, as expected from their assignment to in-plane-polarized a′ vibrations (Table II).

These results confirmed all of the previously suggested vibrational symmetry assignments in **1** and **2**, except for the 735-cm^{-1} peak in **1**, which we were not able to observe starting with the diazide precursor, and the 732-cm^{-1} peak in **2**, which we were able to observe at 729 cm^{-1}, but which was now too weak for a reliable measurement of dichroism. It is not clear whether the weak 735-cm^{-1} peak observed previously for **1** with a different precursor now has a larger bandwidth and is submerged in noise or whether it does not belong to **1**.

The four new vibrational symmetry determinations in **1** and the four new ones in **2** all agree with the vibrational assignments proposed earlier on the basis of MNDO calculations.[3] In particular, the previous concern with the assignment of the out-of-plane CH_2 wag to the 830 -cm^{-1} band, now observed at 831 cm^{-1} with out-of-plane polarization, is removed.

Photoselection on the UV Band of 2. In these experiments, **1** was fully bleached with unpolarized visible light and converted to **2**. Then, **2** was irradiated with linearly polarized 248-nm light whose electric vector was directed along *Z* and partially reconverted to **1**. The polarized IR spectra E_Z and E_Y were then corrected by subtraction of contributions due to species other than **1** and **2** similarly as above. Only the peaks of remaining **2** but not those of the photoproduct **1** showed dichroism.

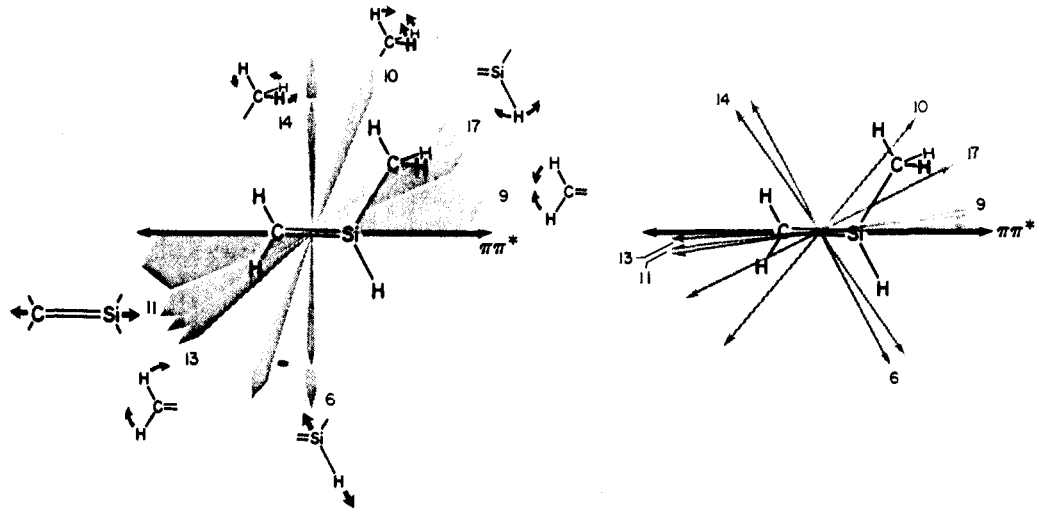

Figure 6. Transition moment directions of in-plane polarized transitions of 1-methylsilene in the UV (black arrows) and IR (grey arrows) regions. Left, measured; right, calculated (MNDO for IR and INDO/S for UV transitions).

This lack of orientation in the product may be due to the large amount of energy that needs to be dissipated during the photochemical process induced by the 248-nm photon; perhaps the molecule tumbles indiscriminately before it cools off. Only a small degree of dichroism would be expected for in-plane polarized bands anyway, since the absorbing transition moment is now not even approximately parallel to either of the two in-plane symmetry axes along which the a_1 and b_2 vibrations of **1** are polarized.

The difference $E_Z - E_Y$ was plotted as shown in Figure 5, and the dichroic ratio d_i was determined for each reproducibly observed transition i.

The above results obtained by photoselection on the visible band of **1** reaffirmed the previously reported[3] out-of-plane or in-plane polarizations of the vibrations in **1** and **2** and provided such assignments for eight additional peaks, but did not open access to any fundamentally new type of information. To the contrary, photoselection on the UV band of **2**, made possible by the use of the new precursor, provides access to information of a type not available before in that it permits a differentiation among the various possible in-plane directions. We were not able to perform such measurements earlier since the precursor used for the previous experiments, dodecamethylcyclohexasilane, as well as the photochemical byproduct, decamethylcyclopentasilane, absorbed too strongly in the 260-nm region.

Although the exact direction of the UV transition moment in 1-methylsilene **2** is unknown, it appears quite safe to assume that this is a $\pi\pi^*$ transition, that it is purely polarized, and that its moment approximately parallels the C=Si bond, perhaps inclined somewhat toward the CH_3 substituent. An INDO/S[16] calculation at an MNDO[17] optimized geometry (assumed planar)[18] suggests that the angle of inclination is only 2.5°. We shall see later that the assumed polarization direction of the 260-nm band is indeed compatible with the polarization results, and this agreement can be taken as support for the $\pi\pi^*$ assignment of this UV transition.

We shall keep x as the axis perpendicular to the CSiC plane and shall now locate the y axis along the absorbing UV transition moment. The z axis will then lie in the CSiC plane. Since the 248-nm absorption is assumed to be purely polarized, nothing distinguishes the orientation of the x and z axes.

While the introduction of the orientation factors in the discussion of the photoselection results for **1** could be viewed as an unnecessary luxury, they will now represent a useful tool in the quantitative analysis of the similar results for **2**. We keep the orientation factors of the three axes, K_y and $K_x = K_z$ (the equality of K_x and K_z follows from the above-noted equivalence of the x and z axes with respect to orientation induced by the photoselection process; it guarantees $K_y = 1 - 2K_z$). We now also define the orientation factor of an arbitrary transition moment direction i firmly tied to the molecular framework, in an entirely analogous fashion: $K_i = \langle \cos^2 i \rangle$. The factors K_i were determined from the dichroism of each observed transition i by using the relation $K_i = d_i/(2 + d_i)$ and are listed in Table II. The relation between K_i and the absolute value of the angle α_i which the ith transition moment forms with the y axis is[13,15]

$$\tan^2 \alpha = \frac{K_y - K_i}{K_i - K_z}$$

We note first that the dichroism of the out-of-plane polarized transition at 614 cm^{-1} is positive, proving that the absorbing UV moment indeed lies in the CSiC plane. The analysis can now be performed with two limiting assumptions.

(i) If there is no error in the dichroic ratio measured for the 614-cm^{-1} vibration, we have $K_x = K_z = K_{614} = 0.38$ and therefore $K_y = 0.24$. The equation for α_i becomes

$$|\alpha_i| = \tan^{-1} [(K_i - 0.24)/(0.38 - K_i)]^{1/2}$$

The results for the seven in-plane polarized transitions for which K_i's were obtained are listed in the next to last column (i) of Table II. Two of them, the one at 811 cm^{-1} and the doublet at 2182 and 2187 cm^{-1}, are polarized along z, since within our experimental error $K_{811} = 0.39$ and $K_{2182} = 0.38$ are both equal to K_x.

(ii) If the accuracy of the dichroic ratio observed for the 614-cm^{-1} transition were subject to doubt, one could assume instead that the $\pi\pi^*$ transition, the Si=C stretching vibration at 989 cm^{-1} (ν_9), and the CH_2 scissoring vibration at 1296 cm^{-1} (ν_7) are all polarized along the Si=C bond. This is compatible with the observed K values for the two vibrations, which are equal within experimental error. Taking $K_y = 0.26$, we obtain $K_x = K_z = 0.37$ and

$$|\alpha_i| = \tan^{-1} [(K_i - 0.26)/(0.37 - K_i)]^{1/2}$$

The results obtained for the in-plane polarized transitions are given in the last column (ii) of Table II.

The two sets of values for α_i correspond to reasonable limits for the K values, keeping the assumption of pure polarization for

(16) Ridley, J.; Zerner, M. *Theor. Chim. Acta* **1973**, *32*, 111.
(17) Dewar, M. J. S.; Ford, G. P. *J. Am. Chem. Soc.* **1977**, *99*, 1685.
(18) A fully optimized MNDO geometry is pyramidal at the Si atom.[3] As discussed earlier,[3] this appears to be an artifact due to the MNDO model, since high-quality ab initio calculations all agree that in silenes the geometry at silicon should be planar (for a review see: Raabe, G.; Michl, J. *Chem. Rev.* **1985**, *85*, 419). In order to obtain meaningful polarization directions we have enforced planarity in the present set of calculations. This causes the appearance of an imaginary frequency for the Si–H out-of-plane bend and has essentially no effect on the computed frequencies of any other vibrations.

the absorbing UV transition, and we take them to bracket the correct answers. In view of the limited accuracy with which the K_i values can be measured, we estimate that these limits are subject to an error of about 5–10° for the larger angles and up to 20–30° for those values of α which are close to zero. In particular, we cannot exclude that both transitions 9 (ν_7) and 11 (ν_9) have transition moments nearly parallel not only to each other but also to the $\pi\pi^*$ transition. Taking the $\pi\pi^*$ transition to be parallel to the Si=C bond, as suggested by the INDO/S calculation which predicts a deviation of 2.5°, permits us to tie the observed transition moment directions to the molecular framework, except that only the absolute values $|\alpha_i|$ are available. In order to assign the signs of these angles, we rely on MNDO calculations (Table II, Figure 6). Their results are those expected by common sense: the Si=C stretch (no. 11, ν_9) and the CH_2 scissoring (no. 9, ν_7) transitions are polarized almost exactly parallel to the Si=C bond, the Si—H stretch (no. 6, ν_5) is polarized parallel to the Si—H bond and the Si—H bend (no. 17, ν_{13}) perpendicular to it, while the symmetrical CH_3 deformation (no. 10, ν_8) is polarized parallel to the Si—C bond and the in-plane CH_3 rock (no. 14, ν_{11}) perpendicular to it. Only the result for the in-plane CH_2 bend, calculated to mix fairly heavily with the SiH bend, is counterintuitive: this vibration is calculated to be polarized nearly parallel to the Si=C bond.

The choice of signs suggested by comparison with the MNDO calculations is shown in Table II. The qualitative agreement between the measured and calculated IR transition moment directions can be seen in Table II and in Figure 6 and is quite satisfactory. Quantitative agreement leaves much to be desired, and it is not obvious which part of the discrepancies is due to experimental inaccuracies and which part to deficiencies of the MNDO model. In particular, although the calculated and measured order of the angles $|\alpha_i|$ agree very well, none of the calculated values are as close to 90° as the measurement suggests.

Still, it is quite remarkable to note how well the approximate experimental IR polarization directions reflect the nature of the vibrational motions assigned previously[3] to the individual IR peaks.

Conclusions

Dimethyldiazidosilane represents a superior photochemical precursor to matrix-isolated dimethylsilylene (**1**) and 1-methylsilene (**2**). Its use permitted us to perform photoselection experiments which established one vibration of **1** as out-of-plane (b_1) and five as in-plane (a_1 or b_2) polarized and four vibrations of **2** as out-of-plane polarized (a″). Most remarkably, a combination of photoselection on two different electronic transitions permitted the assignment of approximate polarization angles to seven in-plane (a′) polarized vibrations of **2**. This represents a potentially very powerful way of characterizing matrix-isolated species. All of the results are in agreement with the IR assignments proposed previously,[3] with MNDO calculations, and with the proposed structures of **1** and **2**. As outlined in more detail elsewhere,[10] we believe that the recent criticism[5,6] of the structural assignment of **1** is unfounded.

Acknowledgment. This work was supported by Air Force Office of Scientific Research Grants F49620-83-C-0044 and 84-0065. One of us (G.R.) is grateful to the Studienstiftung des Deutschen Volkes for a postdoctoral fellowship. We are grateful to Dr. George Radziszewski for help with some of the experiments and to Professor A. C. Arrington (Furman University, Greenville, S.C.), who performed some of the initial work during his sabbatical leave at the University of Utah.

Registry No. **1**, 6376-86-9; **2**, 38063-40-0; dimethyldiazidosilane, 4774-73-6.

The Thermochemistry and Dissociation Dynamics of Internal-Energy-Selected Pyrazole and Imidazole Ions†

Jan Main-Bobo,‡ Susan Olesik,‡ William Gase,‡ Tomas Baer,*‡ Alexander A. Mommers,§ and John L. Holmes§

Contribution from the Department of Chemistry, University of North Carolina, Chapel Hill, North Carolina 27514, and the Department of Chemistry, Ottawa University, Ottawa, Canada.
Received August 26, 1985

Abstract: The two five-membered ring isomers of $C_3H_4N_2^{+\cdot}$, pyrazole and imidazole, have been investigated by photoionization mass spectrometry and photoelectron photoion coincidence spectroscopy. New ionization potentials of 9.25 eV for pyrazole and 8.81 eV for imidazole have been determined from the photoionization efficiency onsets. The dissociation rates of energy-selected ions to the products $CH_2CNH^{+\cdot}$ + HCN and $HCNH^+$ + $C_2H_2N\cdot$ have been measured. By comparing these rates with those expected from the statistical theory (RRKM/QET), the 0 K onsets for the dissociation of pyrazole ions have been found to be 11.77 eV ($CH_2CNH^{+\cdot}$) and 11.80 eV ($HCNH^+$). These exceed the thermochemical dissociation limits by 1.25 and 0.85 eV, respectively. The reverse activation barriers are consistent with the measured kinetic energy releases, which are large and nonstatistical. The different dissociation rates and the different branching ratios to the various products demonstrate that pyrazole and imidazole ions do not isomerize to a common structure prior to dissociation. Finally, evidence is presented that shows that electron impact ionization and photoionization produce ions in different manners, which causes the H loss from metastable parent ions to be very intense in electron impact but to be essentially absent in photoionization.

The field of polyatomic ion dissociation dynamics and gas-phase ion structures is an area rich in surprises. Often, the most stable ionic isomer is not stable as a neutral species.[1-5] In addition, some ions can rearrange to lower energy isomeric structures with remarkable facility.[6-10] Among these are the $C_4H_6^{+\cdot}$ isomers:[6] the butadienes, butynes, cyclobutene, and methylenecyclopropane.

† This work has supported by grants from the National Science Foundation and the Department of Energy.
‡ University of North Carolina.
§ Ottawa University.

(1) Holmes, J. L.; Lossing, F. P. *J. Am. Chem. Soc.* **1980**, *102*, 3732.
(2) Burgers, P. C.; Holmes, J. L. *Org. Mass Spectrom.* **1984**, *19*, 452.
(3) Meisels, G. G.; Hsieh, T.; Gilman, J. P. *J. Chem. Phys.* **1980**, *73*, 4126.
(4) Berkowitz, J. *J. Chem. Phys.* **1978**, *69*, 3044.
(5) Holmes, J. L.; Terlouw, J. K. *J. Am. Chem. Soc.* **1979**, *101*, 4973.
(6) Werner, A. S.; Baer, T. *J. Chem. Phys.* **1975**, *62*, 2900.

0002-7863/86/1508-0677$01.50/0